MPGD-based counters of single photons developed for COMPASS RICH-1

(Article begins on next page)

You may also be interested in:

MPGD-based counters of single photons developed for COMPASS RICH-1

M. Alexeev,[a] **R. Birsa,**[a] **M. Bodlak,**[i] **F. Bradamante,**[b] **A. Bressan,**[b] **M. Büchele,**[c]
M. Chiosso,[d] **P. Ciliberti,**[b] **S. Dalla Torre,**[a] **S. Dasgupta,**[a,1] **O. Denisov,**[e] **V. Duic,**[b]
M. Finger,[f,g] **M. Finger Jr,**[f,g] **H. Fischer,**[c] **M. Giorgi,**[b] **B. Gobbo,**[a] **M. Gregori,**[a]
F. Herrmann,[c] **K. Königsmann,**[c] **S. Levorato,**[b,2] **A. Maggiora,**[e] **A. Martin,**[b] **G. Menon,**[a]
K. Novakova,[h] **J. Novy,**[i] **D. Panzieri,**[j] **F.A. Pereira,**[k] **C.A. Santos,**[k] **G. Sbrizzai,**[b]
P. Schiavon,[b] **S. Schopferer,**[c] **M. Slunecka,**[f,g] **F. Sozzi,**[a] **L. Steiger,**[h] **M. Sulc,**[l]
F. Tessarotto[a] **and J.F.C.A. Veloso**[k]

[a]*INFN, Sezione di Trieste,*
 Trieste, Italy

[b]*INFN, Sezione di Trieste and University of Trieste,*
 Trieste, Italy

[c]*Universität Freiburg, Physikalisches Institut,*
 Freiburg, Germany

[d]*INFN, Sezione di Torino and University of Torino,*
 Torino, Italy

[e]*INFN, Sezione di Torino,*
 Torino, Italy

[f]*Charles University, Prague, Czech Republic*

[g]*JINR, Dubna, Russia*

[h]*Research Centre for Special Optics and Optoelectronic Systems (TOPTEC), Institute of Plasma Physics,*
 Academy of Sciences of the Czech Republic,
 Turnov, Czech Republic

[i]*INFN, Czech Technical University,*
 Prague, Czech Republic

[j]*INFN, Sezione di Torino and University of East Piemonte,*
 Alessandria, Italy

[1]On leave from Matrivani Institute of Experimental Research and Education, Kolkata
[2]Corresponding author.

[k]*I3N - Physics Department, University of Aveiro,*
 Aveiro, Portugal
[l]*Technical University of Liberec,*
 Liberec, Czech Republic

E-mail: stefano.levorato@ts.infn.it

ABSTRACT: In fundamental research, gas detectors of single photons are a must in the field of Cherenkov imaging techniques (RICH counters) for particle identification in large momentum ranges and with wide coverage of the phase space domain. These counters, already extensively used, are foreseen in the setups of future experiments in a large variety of fields in nuclear and particle physics. The quest of novel gaseous photon detector is dictated by the fact that the present generation of detectors has unique characteristics concerning operation in magnetic field, low material budget and cost, but it suffers of severe limitations in effective efficiency,[3] rates, life time and stability, discouraging their use in high precision and high rate experiments. We are developing large size THick GEM (THGEM)-based detector of single photons. The R&D program includes the complete characterization of the THGEM electron multipliers, the study of the aspects related to the detection of single photons and the engineering towards large size detector prototype. Our most recent achievements include: dedicated studies concerning the ion back-flow to the photo-cathode; relevant progress in the engineering aspects, in particular related to the production of large-size THGEMs, where the strict correlation between the local gain-value and the local thickness-value has been demonstrated the operation of a 300 mm $\times$ 300 mm^2 active area detector at the CERN PS T10 test beam; the introduction of a new hybrid detector architecture offering promising indication, which is formed by a THGEM layer which acts as CsI support and pre-amplification device followed by a MICROMEGAS multiplication stage. The general status of the R&D program and the recent progress are reported

KEYWORDS: Hybrid detectors; Micropattern gaseous detectors (MSGC, GEM, THGEM, RETHGEM, MHSP, MICROPIC, MICROMEGAS, InGrid, etc); Electron multipliers (gas); Photon detectors for UV, visible and IR photons (gas) (gas-photocathodes, solid-photocathodes)

---

[3]The effective efficiency is here defined as the combination of the effective photon detection efficiency and the efficiency of counting single photo electron pulses above threshold. The latter is critically dependent on the detector gain and on the threshold of the readout electronics, in view of the typical exponential distribution of the single electron pulses.

Contents

1 Introduction

Nowadays, the Cherenkov imaging technique for Particle IDentification (PID) has been established as a robust, reliable experimental approach thanks to the use in several experiments. They are used and foreseen in the experimental apparata of several future research programmes.

The effectiveness of visible and UV single photon detection is at the basis of the success of these counters. So far, only vacuum-based detectors and gaseous photon detectors have been adopted. Other photon detectors being developed are interesting only for applications in the far future. Gaseous photon detectors are still the only available option to instrument large ($\approx m^2$) detection surfaces when insensitivity to magnetic field, low material budget, and affordable costs are required.

The present generation of gaseous photon detectors, namely MWPC [1], where a cathode plane is formed by a Printed Circuit Board (PCB) segmented in pads and coated with a CsI film, adopted in several experiments (NA44 [2], HADES [3], COMPASS [4], STAR [5], JLab-HallA [6] and ALICE [7]) exhibits some performance limitations: ageing, causing a severe decrease of the quantum efficiency after a collected charge of the order of some mC/cm^2 [8], feedback pulses with a rate increasing at large gain-values, and long recovery time (about 1 day) after an occasional discharge in the detector. These limitations are related to the photon feedback from the multiplication region and to the bombardment of the CsI photocathode film by the positive ions generated in the multiplication process. They impose to operate at low gain (a few times 10^4), resulting in two relevant consequences: the efficiency of single photoelectron detection is reduced and rate limitations are present. Moreover, in these detectors the signal formation is intrinsically slow.

There is a clear quest for novel gaseous photon detectors with advanced characteristics, namely intrinsically fast signals and reduced photon and ion back flow to operate at larger gains and to ensure longer detector life-time.
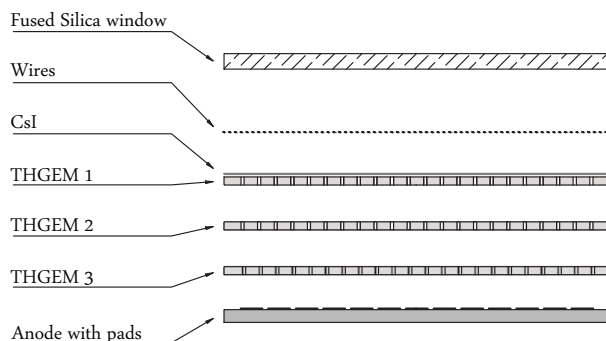
Figure 1. The closed structure arrangement for a micro pattern gaseous based electron multiplier (THGEM in this particular case), built of three electrode layers. UV photon sensitivity can be achieved with a photon converting CsI deposit on the first THGEM electrode.

2 THGEM as single photon detector

Within the RD51 collaboration, which aims to the development of Micro Pattern Gaseous Detector technologies, in 2009 we have started an intense R&D activity aiming to pin out the best candidate to improve COMPASS RICH-1 detector capabilities by replacing the MWPC based photon detector system with a new technology. It is clear that the critical issue of the photon feedback can find a potential solution in the use of a closed geometry structure, where the photo converting layer can not be reached by the photons generated in the multiplication process (see figure 1 as example), in addition with a multilayer structure of electron multipliers a good fraction of the ions can be trapped by the intermediate layers provided the proper choice of the electric fields; finally the possibility to use several multiplication stages allows for high gain operation.

THick GEMs (THGEM) [9], introduced in parallel by several groups about ten years ago, are electron multipliers derived from the GEM [11] design, by scaling the geometrical parameters and changing the production technology. The possibility to produce large size devices at affordable cost despite the few millions holes per square meter, their intrinsic mechanical stiffness, their robustness against damages produced by electrical discharges and the possibility to operate them in magnetic field thanks to the reduced gaps between each multiplier stage, are the appealing features that persuaded us to their use as single photon detector candidates for the RICH-1 upgrade.

The basic architecture of the THGEM-based photon detector that we propose consists in multiple, typically triple, THGEM layers, where the top face of the first layer is coated with a CsI film and acts as a reflective photocathode. The electron multiplication takes place in the THGEM holes thanks to the dipole electric field obtained biasing the two PCB faces. A plane of drift wires defines the drift electric field above the first THGEM layer. The field between two THGEM layers acts as a transfer field; an induction field is applied between the bottom face of the last THGEM and the anode electrode. The signals are collected at the anode plane, formed by a PCB segmented in pads. A large variety of different small THGEMs types, $30mm \times 30mm$ active area, have been extensively studied [10, 12] and the results of a broad campaign of tests performed to characterize and evaluate their performance have been presented and discussed in [13]. The reader is referred to the cited publications and the reference therein for further details.

Electrostatic calculations using COMSOL Multiphysics[1] and simple simulation exercises using ANSYS[2] and GARFIELD[3] played an important role for reaching a qualitative understanding of the observed THGEM behaviour. Photoelectron extraction and collection efficiencies have been studied for various THGEM parameters, field configurations and gas mixtures, leading to the following choices: use of pure methane or methane-rich mixtures (Ar/CH4 70/%30) to reduce the photoelectron backscattering effects, operate with an electric field at the CsI surface larger than 1 kV/cm to grant efficient photoelectron extraction, use a ratio between hole diameter and pitch of 0.5, use a CsI coated THGEM with 0.4 mm thickness and very small (below 10 μm) or no rim.

A THGEM based photon detector does not suffer from photon feedback while the ions generated in the multiplication process can easily reach the photocathode surface following back the electric field lines. Measurement performed in laboratory test confirm the IBF fraction reaching the photocathode to be about 30% of the total ions generated, the remaining 70% is collected by the intermediate layers [15].

For detector operations at high gain of 10^5, and to avoid instabilities, the ion feedback must be reduced at few % level.

Resuming the pioneering procedure by F. Sauli and collaborators [14] and arranging the THGEMs so that THGEM$_1$ and THGEM$_3$ to have aligned holes while there is a complete misalignment of the holes of THGEM$_2$ respect to THGEM$_1$ and THGEM$_3$ it is possible to reduce the IBF to values below 5%; this working condition is obtained thanks to the interplay of the electric field between the THGEM electrodes E$_{TR_{1,2}}$ and the corresponding dipole field. The values of E$_{TR_1}$=1kV/cm and E$_{TR_2}$=4 kV/cm grant for a IBF 3% with a measured effective gain of 2×10^5. Comparing the two extreme configurations: completely aligned and completely misaligned holes of THGEM$_2$, for the same biasing electrode voltage the effective gain is reduced by 40% [15]. This gain loss can be recovered increasing the voltage across the last THGEM multiplier stage.

## 3   Test Beam result of large size single photon detectors

During the fall of 2012 a large size detector has been operated at the T10 beam line at CERN. The detector consists of three THGEM with 0.4 mm holes diameter and 0.8 mm pitch; the CsI coated one is 0.4 mm thick while the remaining 0.8 mm thick. The distance between the 576 12mm$\times$12mm pad segmented anode and the first THGEM is 2.5 mm, the distance between the THGEMs is 3mm and 5mm separate the photo sensitive layer and the drift wire plane. Each THGEM layer is segmented into 6 sectors 300 mm$\times$ 48 mm electrically separated by 0.8 mm PCB insulation area. The high voltage is distributed by six independent resistive dividers each divider is powered by a dedicated HV channel and it biases 6 THGEM sectors and the corresponding drift wire sector in a cascade-like architecture.[4] The detector is operated in Ar/CH$_4$ 60/40% mixture.

---

[1]www.comsol.com

[2]www.ansys.com

[3]http://garfield.web.cern.ch/garfield/

[4]Each layer is segmented into 6 different sectors: for example each sector of the drift plane is labelled with D_i where i runs from 1 to 6. The CsI coated THGEM layer T_1 is segmented accordingly and is labelled $T_{1,i}$, its corresponding bottom is then labelled $B_{1,i}$. The same applies for THGEM$_2$ and THGEM$_3$. Each resistive divider is biasing the whole set of electrodes built by $D_i + T_{1,i} + B_{1,i} + T_{2,i} + B_{2,i} + T_{3,i} + B_{3,i}$
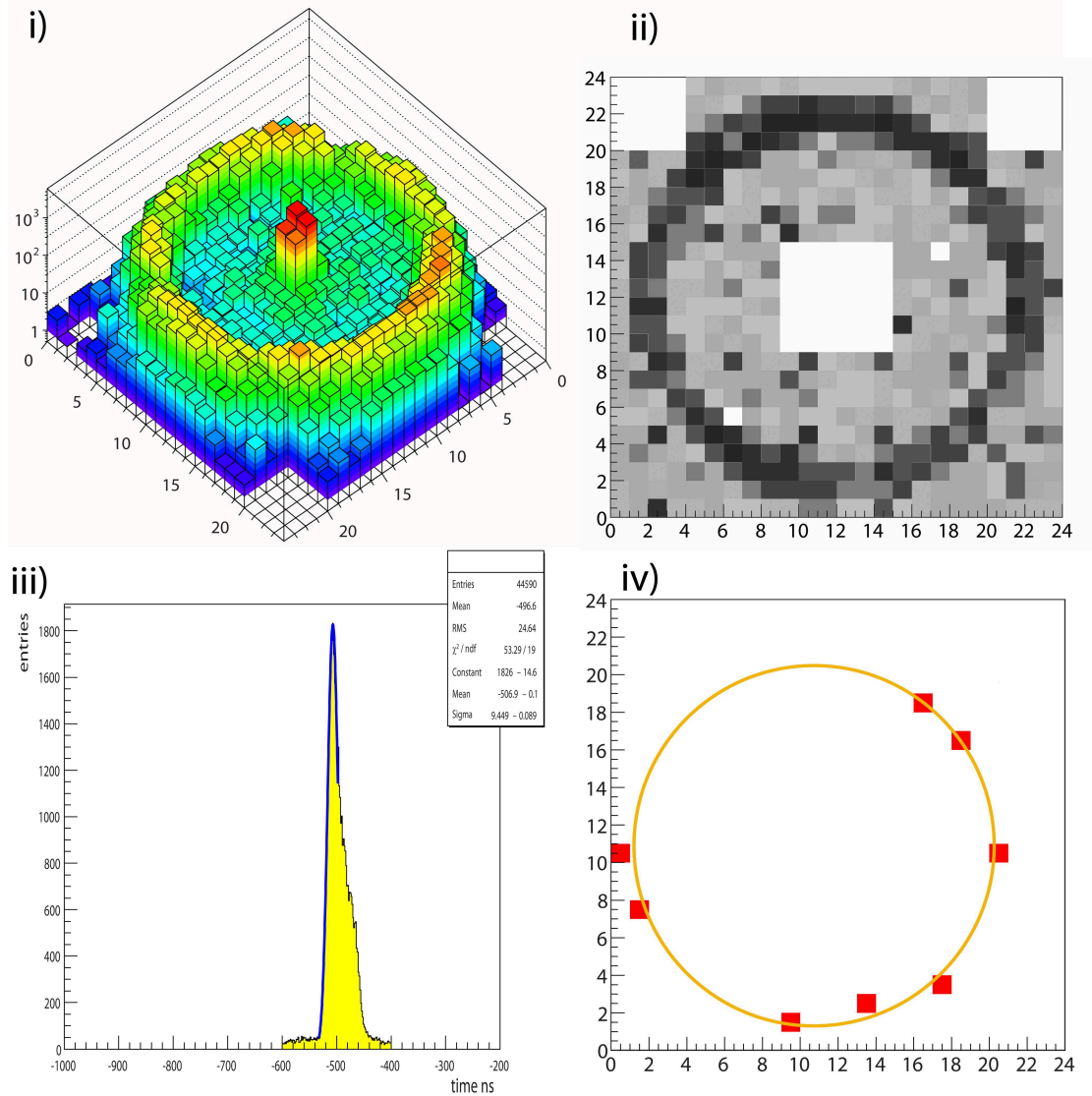
Figure 2. i) Superposition of events, the Cherenkov corona is clearly visible as well as the beam events in the centre of the corona, which by crossing a conical shaped fused silica radiator generates the Cherenkov light. ii) The same picture as in figure i) but excluding beam hits. iii) Time distribution of the Cherenkov detected events: the r.m.s. is ≈ 10 ns. iv) Single event hits and superimposed the expected Cherenkov ring.

The detector read out is based on the MAD-4 front-end chip and the F1 TDC chip [16], the 120 ps digitisation unit allows to exploit the detector performance.

Figure 2-i) illustrates the superposition of Cherenkov photon events generated by charged particles at $\beta \approx 1$. The light is produced by particles crossing a quartz conical radiator positioned in front of the first THGEM layer. The light emitted generates a corona of photons, 270 mm of diameter, which is converted by the CsI layer. The spot located at the corona centre is generated by the beam particles. Figure 2-ii) illustrates the same set of events in figure 2-i) but excluding the beam hits. Figure 2-iii) shows the time distribution of the Cherenkov events in 2-ii). The Gaussian
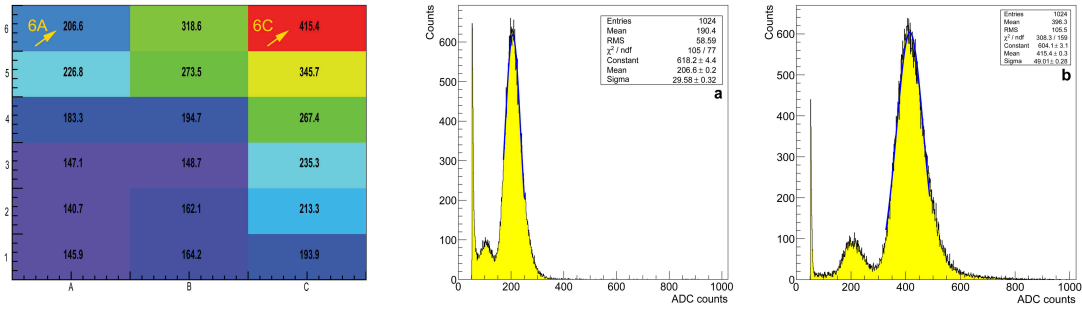
Figure 3. Left: gain measured in ADC channels for the 18 electrically independent sectors of a large 0.8 mm thick THGEM detector when the same biasing voltage of 1825 volt is applied between the two electrode surfaces. Centre, *(a)*: ^{55}Fe spectrum for sector 6A, right *(b)* ^{55}Fe spectrum for sector 6C. The Ar escape peak and the full energy peak are clearly visible.

fit of the distribution has a r.m.s. ≈ 10ns. The detector shows performance very similar to the small prototypes ones tested in previous test beam exercises.

Figure 2-iv) illustrates a single particle event: 8 single photons are detected. The amount of light generated by each crossing particle grants the single photon regime.

The full detector was operated in stable working condition at gain of 2×10^4 while it was possible to operate one sector at gain values of 2×10^5.

4 Large size THGEM production issues

Despite the fact that large area THGEMs can be easily produced by industry at moderate cost (typically around 1 Euro every 1000 holes), the production of large area THGEMs of high quality and uniformity of response is challenging. A set of systematic tests, described in [17], permitted to pin out the origin of the limit for the maximum stable gain of the large THGEM-based PD: local variations of the THGEM thickness and microscopic defects (sharp edges or scratches) on the copper edge of some holes. Both effects are proportional to the number of holes, which is 100 times larger on the large size THGEMs with respect to the small ones. The thickness uniformity of the PCB material used for THGEM production has been measured for a large number of pieces and maps of the local gain of the THGEMs clearly show a strict correlation between the local thickness and the measured gain, which could show variations up to a factor 3 for regions with 10% thickness difference. Figure 3 left illustrates the gain uniformity distribution for a 0.8 mm thickness THGEM when a biasing voltage of 1825 V is applied between the two electrode surfaces. The ratio between the maximum and the minimum measured gain for the specific applied voltage reaches nearly a value of 3, as it can be computed by comparing the top right and bottom left corners (6C and 1A). When the detector thickness is taken into account the correlation between the two quantities is evident: the large gain values are obtained for the thinner area $700\mu m$ (position 6C) to be compared with the $780\mu m$ (position 1A). Figure 3a and 3b present examples of the amplitude spectra: after the noise peak at low ADC counts two Gaussian peaks can be observed: they correspond to the characteristic Ar escape peak at 2.9 keV in addition to the full energy peak at 5.9 keV: the gain

is obtained from the Gaussian fit of the full energy peak. A significant gain variation can be seen between the two different positions of the same electrode sector.

Carefully selecting the most uniform areas of the raw material (with 2% thickness tolerance), it was possible to obtain 300 mm × 300 mm THGEMs with a ratio between maximum and minimum measured gain 1.5. Specific treatments (polishing, micro-etching or polyurethane coating) have been proposed and successfully applied by the CERN TS-DEM-PMT team after the industrial production and the first tests. The best results have been obtained using a similar treatment [17], developed for this R&D project, consisting in a careful polishing process with thin-grain pumice powder and a long, mild chemical etching by a highly basic aqueous solution of Sonica PCB[5] in ultrasonic bath. The newly produced large THGEMs can operate at higher voltage and provide stable and uniform response.

5 A new architecture based on two MPGD detectors: MICROMEGAs and THGEMs

One of the most complicated and challenging operation aspects of the triple THGEMs photon detector is the IBF reduction. An alternative way of suppressing the IBF comes from natural suppression the ions in the multiplication process of a MICROMEGAS [18].

The two MPGD structures can be coupled exploiting the advantages of the two architectures. The hybrid structure makes use of a Bulk MM produced at CERN. The Micromesh-anode distance is 128 μm, the spacer diameter and pitch is 300 μm and 2 mm respectively, see figure 4. The micromesh is a stainless steel grid of 18 μm diameter woven wires separated by a distance of $\approx 80\mu$m. 5 mm separate the mesh from the bottom layer of the THGEM, characterised by 0.4 mm holes, 0.8 mm pitch and 0.4 mm thickness and no rim. The wires of the drift plane placed above the THGEM to define the electric field have 100 μm diameter and to 2 mm pitch; the plane is at a distance of 20 mm from the top THGEM face. The principle scheme as well as the details of the hybrid detector can be seen in figure 4. The detector fields have been optimised, via dedicated tests: no electron loss is observed for a transfer field above 0.8 kV/cm; the ratio of the fields above and below the Micomegas mesh is kept around 40 or larger. Different gas mixtures have been used Ar/C0$_2$ 70/30 and Ar/CH$_4$ based, no maximum gain dependence on the Ar/CH$_4$ ratio has been observed.

X-Ray from an ^{55}Fe source spectra have been used to study the detector performance. The signals are processed by a read-out chain composed by a CREMAT CR110[6] preamplifier, an Ortec 672[7] amplifier and an MCA8000A digitizer by Amptek[8].

A non negligible advantage in the use of the hybrid structure comes also from the reduced number of independent electrodes to power (42 for a triple THGEM detector) but mostly from the reduced value of the HV to supply: for CH$_4$ rich mixtures a triple THGEM detector requires almost 10kV while for the hybrid it drops below 5kV. This reduction simplifies several production aspects. Clearly a lower powering high voltage corresponds to a reduced accumulated charge at the detector level: in case a discharge occurs the probability of damage is reduced.

---

[5]http://www.soltec.it

[6]Cremat, Inc., Watertown, Massachusset, U.S.A.

[7]ORTEC Advanced Measurement Technology, Inc, Oak Ridge, Tennessee, U.S.A.

[8]Amptek Inc., Bedford, Massachusset, U.S.A.
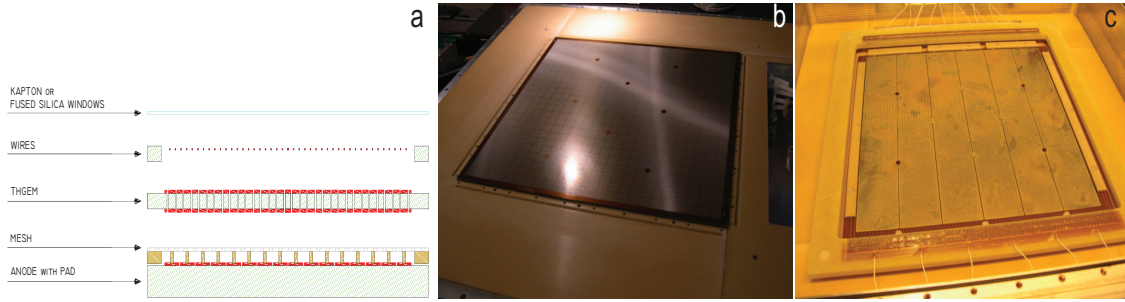
Figure 4. a) typical structure of the Hybrid detector. The CsI is deposited on the first THGEM layer. b) The 300×300 mm^2 bulk Micromega mesh glued on its support frame. c) the full detector assambled, the THGEM sectors and the wire plane are visible.
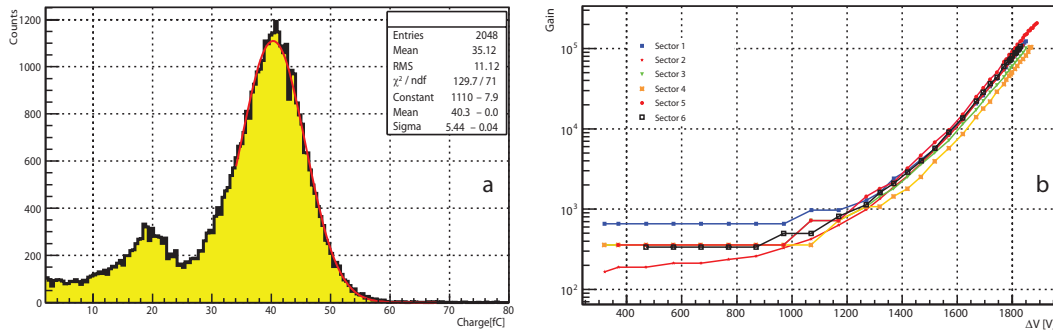
Figure 5. Amplitude spectra obtained with the hybrid detector prototype using the ^{55}Fe source in in Ar/CH$_4$ 3070; estimated gain: 1.3×10^3. Right: gain as function of ΔV for V_{mesh} =640 V, for each of the the six THGEM Sectors

Before assembling the hybrid detector, both the MM and the THGEM detectors have been characterized. In particular the MM exhibits a gain uniformity at 12% level figure 5 top shows the spectrum of the ^{55}Fe source collected using the hybrid detector in Ar/CH$_4$ 30:70. The voltage applied to the mesh electrode is V_{mesh} = 0.55 kV, the transfer field is E$_{trans}$ = 0.900 kV/cm, the bias voltage across the THGEM layers is ΔV = 2 kV, the drift field is E$_{drift}$ = 1.5 kV/cm. The corresponding gain is 1.5×10^3. The full detector has been tested to check the performance of the 6 sectors as illustrated in figure 5 where for 0.64 kV fixed voltage of the mesh the gain of the detector is measured varying the ΔV across the THGEM multiplier. All the sectors respond in a similar way. It has to be noticed that up to 1kV ΔV, the whole multiplication is in the MM stage. Increasing the voltage the multiplication starts also inside the THGEM holes, reaching for all the sector a maximum gain of 1.2×10^5, apart one where the 2.2×10^5 is achieved. It is important to remark that the hybrid detector can also profit from the use of a resistive anode [19] with two major advantages: the sensitive readout electronics is decoupled from the direct current during occasional discharges,

protecting it; the spark energy is reduced and the dead-time due to the detector discharges is almost completely suppressed, introducing the possibility to operate in high rate environments [19].

6 The Compass RICH-1 upgrade

COMPASS RICH-1 is in operation since 2001. In its original version it used eight MWPCs with 576 mm × 1152 mm active area, equipped with CsI-coated photocathodes and pad readout. In spite of their good performance, MWPC-based PDs present intrinsic limitations as mentioned before in section 1. To improve the RICH-1 figure, a set of new, high performing photon detectors with an active area of 576 mm × 576 mm will be provided for the upgrade of COMPASS RICH-1. They are based on the Hybrid scheme, whose working principle, performance and feasibility have been proven and illustrated beforehand. A challenging operation is represented by the integration of the new photon detection system with the existing one, for this reason a full-size prototype is presently being designed and the engineering problems are being studied. It is foreseen in fact to equip the COMPASS RICH-1 with the new PD system for the 2016/17 data taking runs.

References

[1] F. Piuz, *Ring Imaging Cherenkov systems based on gaseous photo-detectors: Trends and limits around particle accelerators*, *Nucl. Instrum. Meth.* **A 502** (2003) 76.

[2] J. Humanic et al., *Recent results from the CERN NA44 experiment*, *Int. J. Mod. Phys.* **A 16** (2001) 1257.

[3] HADES collaboration, K. Lapidus et al., *The HADES-at-FAIR project*, *Phys. Atom. Nucl.* **75** (2012) 589.

[4] COMPASS collaboration, P. Abbon et al., *The COMPASS experiment at CERN*, *Nucl. Instrum. Meth.* **A 577** (2007) 455 [`hep-ex/0703049`].

[5] STAR collaboration, A. Braem et al., *Identification of high p_T particles with the STAR-RICH detector*, *Nucl. Instrum. Meth.* **A 499** (2003) 720.

[6] F. Garibaldi et al., *A proximity focusing RICH detector for kaon physics at Jefferson Lab Hall A*, *Nucl. Instrum. Meth.* **A 502** (2003) 117;
M. Iodice et al., *Performance and results of the RICH detector for kaon physics in Hall A at Jefferson Lab*, *Nucl. Instrum. Meth.* **A 553** (2005) 231 [*Erratum ibid.* **A 556** (2006) 644].

[7] A. Di Mauro et al., *The VHMPID RICH upgrade project for ALICE at LHC*, *Nucl. Instrum. Meth.* **A 639** (2011) 274.

[8] A. Braem et al., *Results from the ageing studies of large CsI photocathodes exposed to ionizing radiation in a gaseous RICH detector*, *Nucl. Instrum. Meth.* **A 553** (2005) 187;
H. Hoedlmoser et al., *Long term performance and ageing of CsI photocathodes for the ALICE/HMPID detector*, *Nucl. Instrum. Meth.* **A 574** (2007) 28.

[9] L. Periale et al., *Detection of the primary scintillation light from dense ar, kr and xe with novel photosensitive gaseous detectors*, *Nucl. Instrum. Meth.* **A 478** (2002) 377 [`physics/0106048`];
P. Jeanneret, *Time Projection Chambers and detection of neutrinos*, PhD 582 thesis, Neuchâtel University (2001);
P.S. Barbeau et al., *Toward coherent neutrino detection using low-background micropattern gas detectors*, *IEEE Trans. Nucl. Sci.* **50** (2003) 1285 [`hep-ex/0212034`];

R. Chechik, A. Breskin, C. Shalem and D. Mormann, *Thick GEM-like hole multipliers: Properties and possible applications*, *Nucl. Instrum. Meth.* **A 535** (2004) 303 [`physics/0404119`].

[10] A. Breskin et al., *A Concise review on THGEM detectors*, *Nucl. Instrum. Meth.* **A 598** (2009) 107 [`arXiv:0807.2026`].

[11] F. Sauli, *GEM: A new concept for electron amplification in gas detectors*, *Nucl. Instrum. Meth.* **A 386** (1997) 531.

[12] M. Alexeev et al., *Detection of single photons with ThickGEM-based counters*, 2012 *JINST* **7** C02014.

[13] M. Alexeev et al., *The quest for a third generation of gaseous photon detectors for Cherenkov imaging counters*, *Nucl. Instrum. Meth.* **A 610** (2009) 174;
M. Alexeev et al., *THGEM based photon detector for Cherenkov imaging applications*, *Nucl. Instrum. Meth.* **A 617** (2010) 396;
M. Alexeev et al., *Micropattern gaseous photon detectors for Cherenkov imaging counters*, *Nucl. Instrum. Meth.* **A 623** (2010) 129;
M. Alexeev et al., *Development of THGEM-based photon detectors for Cherenkov Imaging Counters*, 2010 *JINST* **5** P03009;
M. Alexeev et al., *Progress towards a THGEM-based detector of single photons*, *Nucl. Instrum. Meth.* **A 639** (2011) 130;
M. Alexeev et al., *Detection of single photons with ThickGEM-based counters*, 2012 *JINST* **7** C02014.

[14] F. Sauli, L. Ropelewski and P. Everaerts, *Ion feedback suppression in time projection chambers*, *Nucl. Instrum. Meth.* **A 560** (2006) 269.

[15] M. Alexeev et al., *Ion backflow in thick GEM-based detectors of single photons*, 2013 *JINST* **8** P01021.

[16] P. Abbon et al., *Read-out electronics for fast photon detection with COMPASS RICH-1*, *Nucl. Instrum. Meth.* **A 587** (2008) 371.

[17] M. Alexeev et al., *Progresses in the production of large-size THGEM boards*, 2014 *JINST* **9** C03046.

[18] I. Giomataris et al., *MicrOMEGAs in a bulk*, *Nucl. Instrum. Meth.* **A 560** (2006) 405.

[19] MAMMA collaboration, J. Manjarres et al., *Performances of Anode-resistive MicrOMEGAs for HL-LHC*, 2012 *JINST* **7** C03040 [`arXiv:1202.1074`].